

Seismic critical-angle reflectometry: A method to characterize azimuthal anisotropy?

Martin Landrø*, Norwegian University of Science and Technology, and Ilya Tsvankin, Center for Wave Phenomena, Colorado School of Mines

Summary

Existing anisotropic parameter-estimation algorithms that operate with long-offset data are based on the inversion of either nonhyperbolic moveout or wide-angle AVO (amplitude-variation-with-offset) response. Here, we show that valuable information about anisotropic reservoirs can also be provided by the critical angle of reflected waves.

To explain the behavior of the critical angle, we develop the weak-anisotropy approximation for vertical transverse isotropy and then use Tsvankin’s notation to extend it to azimuthally anisotropic models of orthorhombic symmetry. The P-wave critical-angle reflection in orthorhombic media is particularly sensitive to the parameters $\epsilon^{(1)}$ and $\epsilon^{(2)}$ responsible for the symmetry-plane horizontal velocities in the high-velocity layer. The azimuthal variation of the critical angle for typical orthorhombic models can reach 5–6°, which translates into substantial changes in the critical offset of the reflected P-wave.

The main diagnostic features of the critical-angle reflection employed in our method include the rapid increase of the reflection amplitude at the critical angle and the subsequent separation of the head wave. Analysis of synthetic seismograms generated with the reflectivity method confirms that the azimuthal variation of the critical offset is detectable on wide-azimuth, long-spread data. Critical-angle reflectometry can be used to constrain the dominant fracture directions and, in combination with other methods, to reduce the uncertainty in anisotropic parameter estimates.

Introduction

Long-offset reflection data play an important role in anisotropic velocity analysis because they are recorded for a wide range of angles with the vertical. In particular, nonhyperbolic (long-spread) moveout analysis is used to constrain anisotropy parameters for both VTI (transversely isotropic with a vertical symmetry axis) and azimuthally anisotropic media (e.g., Vasconcelos and Tsvankin, 2004; Tsvankin, 2005). Wide-angle AVO response can provide information about anisotropy that cannot be obtained from conventional analysis of the AVO gradient (e.g., Rüger, 2001).

Here, we suggest another way of employing long-offset reflections by extending to seismology a well-established technique called “ultrasonic critical-angle reflectometry” (Antic and Mehta, 1997). The P-wave velocity in many hydrocarbon reservoirs is higher than that in the cap rock, which leads to critical and post-critical target reflections.

The shift in the critical angle or offset observed on time-lapse data was shown to be helpful in monitoring reservoir production (Landrø et al., 2004). If the medium is azimuthally anisotropic, the critical angle and the corresponding critical offset vary with azimuth, which can be used to identify the vertical symmetry planes of the model and constrain the anisotropy parameters. Seismic critical-angle reflectometry can be particularly efficient in fracture characterization, if it is combined with azimuthal AVO and moveout analysis (e.g., Grechka and Tsvankin, 1999; Gray et al., 2002).

Analytic description of the critical angle

We consider a plane P- or S-wave incident upon a horizontal interface that separates two anisotropic media. If the transmitted wave (P or S) has a higher velocity, for a certain incidence angle (called the critical angle) its group-velocity vector becomes horizontal. For simplicity, we assume that the reflector coincides with a symmetry plane of the reflecting halfspace, so the phase-velocity vector of the transmitted wave at the critical angle is also horizontal. Then the critical phase angle θ_{cr} can be found from Snell’s law:

$$\frac{\sin \theta_{cr}}{V_1(\theta_{cr})} = \frac{1}{V_{hor,2}}, \quad (1)$$

where $V_1(\theta)$ is the phase velocity in the incidence halfspace and $V_{hor,2}$ is the horizontal phase velocity in the reflecting halfspace computed in the vertical incidence plane. The critical angle for a particular wave mode (e.g., PP, SS, or SP) can be obtained by solving equation 1 with the appropriate phase-velocity function $V_1(\theta)$ and the horizontal velocity $V_{hor,2}$. For point-source radiation, the segment of the wavefront orthogonal to the phase direction θ_{cr} is responsible for generating the head wave, which interferes with the reflected wave in the post-critical domain.

VTI media

A concise approximation for the critical angle of P-waves in VTI media can be obtained by linearizing equation 1 in the Thomsen parameters ϵ and δ :

$$\sin \theta_{cr} = n \left[1 - \epsilon_2 + \delta_1 n^2 + (\epsilon_1 - \delta_1) n^4 \right], \quad (2)$$

where the subscripts “1” and “2” denote the incident and reflecting halfspaces, respectively, $n \equiv V_{P0,1}/V_{P0,2}$, and V_{P0} is the P-wave vertical velocity ($V_{P0,2} > V_{P0,1}$). Since $n < 1$, the contribution of anisotropy to the critical angle is controlled primarily by the parameter ϵ_2 responsible for the horizontal P-wave velocity in the reflecting halfspace. If the overburden is isotropic and the velocity ratio n is known, the angle θ_{cr} can be used to estimate ϵ_2 .

Seismic critical-angle reflectometry

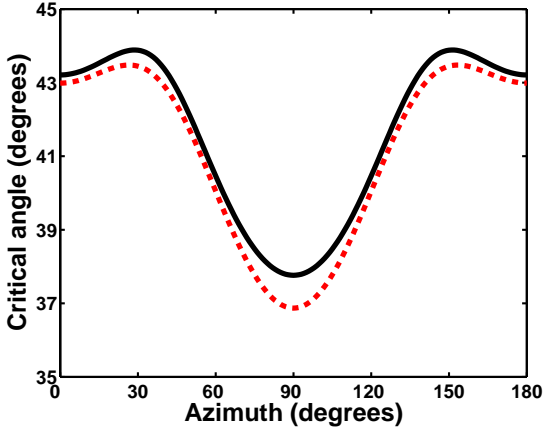


Fig. 1: Critical angle of P-waves as a function of azimuth for an interface between isotropic (incidence) and orthorhombic (reflecting) media. The azimuth ϕ is measured from the symmetry plane $[x_1, x_3]$. The solid curve is the exact angle θ_{cr} from equation 1, the dashed curve is the weak-anisotropy approximation 3. The P-wave velocity in the isotropic halfspace is $V_{P0,1} = 2100$ m/s; the relevant parameters of the orthorhombic halfspace are $V_{P0,2} = 2800$ m/s, $\epsilon_2^{(1)} = 0.25$, $\epsilon_2^{(2)} = 0.1$, and $\delta_2^{(3)} = -0.1$.

Equation 2 can be easily adapted for shear or mode-converted waves by applying the “substitution rule” described by Tsvankin (2005, p. 26). When the incidence medium is anisotropic, the critical offset is determined by the critical group (ray) angle ψ_{cr} that corresponds to θ_{cr} .

Orthorhombic media

Many naturally fractured reservoirs are believed to possess effective orthorhombic symmetry. Existing parameter-estimation methods for orthorhombic media largely rely on multicomponent data (e.g., Grechka et al., 2005), which are not acquired in the bulk of seismic surveys. Suppose an interface separates two orthorhombic media with the same orientation of the symmetry planes, which are aligned with the coordinate planes. The weak-anisotropy approximation 2 can be adapted for this model by making the parameters ϵ and δ functions of the azimuth ϕ with the x_1 -axis (Tsvankin, 2005):

$$\sin \theta_{cr}(\phi) = n \{1 - \epsilon_2(\phi) + \delta_1(\phi) n^2 + [\epsilon_1(\phi) - \delta_1(\phi)] n^4\}; \quad (3)$$

$$\delta(\phi) = \delta^{(1)} \sin^2 \phi + \delta^{(2)} \cos^2 \phi, \quad (4)$$

$$\epsilon(\phi) = \epsilon^{(1)} \sin^4 \phi + \epsilon^{(2)} \cos^4 \phi + (2\epsilon^{(2)} + \delta^{(3)}) \sin^2 \phi \cos^2 \phi. \quad (5)$$

The anisotropy parameters $\epsilon^{(1)}$, $\epsilon^{(2)}$, $\delta^{(1)}$, $\delta^{(2)}$, and $\delta^{(3)}$ are defined in Tsvankin (2005).

In the azimuthal AVO analysis, the best-constrained parameter is the difference between the AVO gradients in

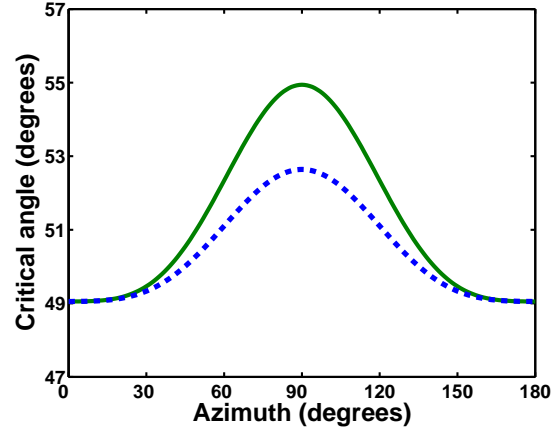


Fig. 2: Critical angle of P-waves obtained from the weak-anisotropy approximation 3 for an interface between orthorhombic (incidence) and isotropic (reflecting) media. The solid curve is computed for the following parameters of the orthorhombic halfspace: $V_{P0,1} = 2100$ m/s, $\epsilon_1^{(1)} = 0.25$, $\epsilon_1^{(2)} = 0.1$, $\delta_1^{(1)} = 0.05$, $\delta_1^{(2)} = -0.1$, and $\delta_1^{(3)} = -0.1$. For the dashed curve, all parameters are the same, except for $\epsilon_1^{(1)} = 0.15$. The P-wave velocity in the isotropic halfspace is $V_{P0,2} = 2800$ m/s.

the vertical symmetry planes (e.g., Rüger, 2001). Likewise, the critical-angle reflectometry can provide an estimate of $\Delta(\sin \theta_{cr}) = \sin \theta_{cr}(0^\circ) - \sin \theta_{cr}(90^\circ)$. When the overburden is isotropic, $\Delta(\sin \theta_{cr})$ can be used to find the difference between $\epsilon_2^{(1)}$ and $\epsilon_2^{(2)}$:

$$\Delta \epsilon_2 \equiv \epsilon_2^{(1)} - \epsilon_2^{(2)} = \frac{\Delta(\sin \theta_{cr})}{n}. \quad (6)$$

If both layers are orthorhombic, equation 5 contains eight anisotropy parameters, which cannot be resolved without additional information.

Numerical examples

The magnitude of the azimuthal variation of the critical angle for typical orthorhombic models and the accuracy of the weak-anisotropy approximation are illustrated in Figures 1 and 2. When the incidence medium is isotropic, the dependence $\theta_{cr}(\phi)$ is controlled by the P-wave horizontal velocity in the reflecting halfspace (equation 1). For the model in Figure 1, $\epsilon_2^{(1)} - \epsilon_2^{(2)} = 0.15$, which translates into a change in θ_{cr} between the symmetry planes that exceeds 5° (equation 6). The extrema of the function $\theta_{cr}(\phi)$, however, do not necessarily coincide with the symmetry-plane directions, if the absolute value of $\delta_2^{(3)}$ is relatively large. The weak-anisotropy approximation is close to the exact solution and correctly reproduces the trend of $\theta_{cr}(\phi)$.

When the incidence halfspace is orthorhombic (Figure 2), the critical angle becomes a function of all five anisotropy parameters responsible for the P-wave velocity above the reflector ($\epsilon_1^{(1)}$, $\epsilon_1^{(2)}$, $\delta_1^{(1)}$, $\delta_1^{(2)}$, and $\delta_1^{(3)}$). The azimuthal dependence of the critical angle in Figure 2 is more pronounced for the model with a larger difference between

Seismic critical-angle reflectometry

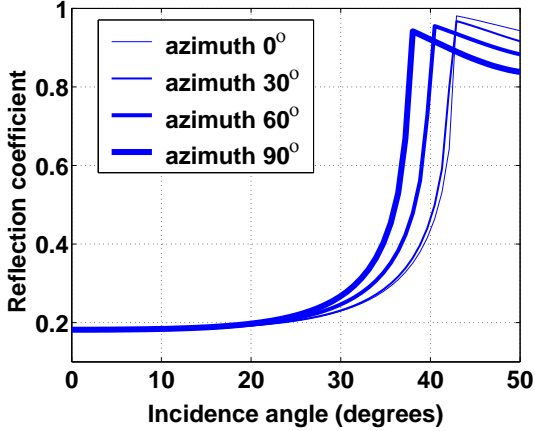


Fig. 3: Real part of the exact reflection coefficient for a plane P-wave computed in four azimuthal directions for an interface between isotropic (incidence) and orthorhombic (reflecting) media. The P- and S-wave velocities in the incidence halfspace are $V_{P0,1} = 2100$ m/s and $V_{S0,1} = 1200$ m/s, the density $\rho_1 = 2.4$ g/cm³. For the reflecting halfspace, $V_{P0,2} = 2800$ m/s, $V_{S0,2} = 1200$ m/s, $\rho_2 = 2.6$ g/cm³, $\epsilon_2^{(1)} = 0.25$, $\epsilon_2^{(2)} = 0.1$, $\delta_2^{(1)} = 0.05$, $\delta_2^{(2)} = -0.1$, $\delta_2^{(3)} = -0.1$, $\gamma_2^{(1)} = 0.28$, and $\gamma_2^{(2)} = 0.15$. The critical angle for this model is plotted in Figure 1.

$\epsilon_1^{(1)}$ and $\epsilon_1^{(2)}$. Variations in the critical angle on the order of 5–6° (Figures 1 and 2) would change the critical offset for deep interfaces by hundreds of meters, which should be detectable on AVO plots.

Reflection coefficient at the critical angle

The critical angle can be identified on surface reflection data by analyzing the amplitude of the reflected wave at near-critical offsets. The real part of the exact P-wave reflection coefficient for an isotropic/orthorhombic interface in Figure 3 varies with azimuth, but has practically the same shape near the azimuthally-dependent critical angle $\theta_{cr}(\phi)$. After a sharp peak at θ_{cr} where its derivative becomes infinite, the real part of the reflection coefficient decreases with angle.

The amplitude of the reflected wave at near-critical incidence, however, is determined not just by the plane-wave reflection coefficient. First, since the amplitude of the reflected wave has a continuous derivative, it should increase beyond θ_{cr} . Second, the reflected wave in the post-critical domain undergoes rapid phase changes and interferes with the head wave. As confirmed by the exact synthetic seismograms below, the critical angle is close to the point of the fastest amplitude increase of the reflected wave, with the amplitude peak shifted toward post-critical offsets.

Synthetic test using reflectivity modeling

The method was tested on synthetic reflection data computed for a model that includes an orthorhombic layer beneath an isotropic medium (Figure 4). The seismograms

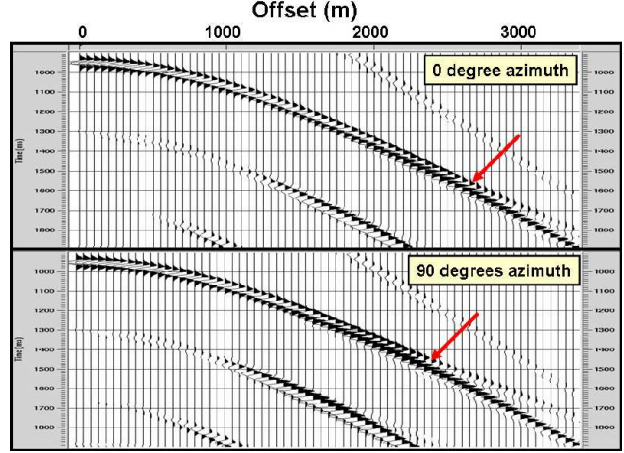


Fig. 4: Synthetic seismograms of the vertical displacement for the wavefield reflected from the top of an orthorhombic layer. The sources and receivers are placed in an isotropic halfspace; the model parameters are the same as in Figure 3. The time axis runs from 900 ms to 1900 ms.

were generated with the anisotropic reflectivity method, which produces exact 3D wavefields for horizontally layered media. We estimated the critical angle for the PP reflection from the top of the orthorhombic layer (see the arrows). For both azimuths in Figure 4, there is a clearly visible head wave splitting off from the reflected wave. The separation of the head wave (marked by the arrows) occurs at a smaller offset for the azimuth $\phi = 90^\circ$, which is indicative of a decrease in the critical angle. The point of the fastest amplitude increase on the AVO curves (Figure 5) yields the critical angle close to 43° for $\phi = 0^\circ$ and 38.5° for $\phi = 90^\circ$.

The estimated critical angle in Figure 6 is close to the exact value for the full range of azimuths. Assuming that the vertical-velocity ratio is known, $\theta_{cr}(\phi)$ can be inverted for all three relevant parameters of the orthorhombic medium – $\epsilon_2^{(1)}$, $\epsilon_2^{(2)}$, and $\delta_2^{(3)}$. If the offset range is sufficiently wide, the horizontal velocity in the orthorhombic layer and the parameters $\epsilon_2^{(1)}$, $\epsilon_2^{(2)}$, and $\delta_2^{(3)}$ can also be estimated from the linear moveout of the head wave.

Discussion

Implementation of critical-angle reflectometry requires considering several important practical issues. First, the critical-angle reflection can be recorded only if there is a significant velocity increase at the top or bottom of the reservoir. Second, the method has to operate on wide-azimuth, long-offset data that include the critical reflected ray from the target. Third, the critical-angle event may be obscured by the overburden noise train, which can be partially attenuated by such techniques as F-K filtering.

Furthermore, quantitative analysis of critical-angle measurements faces a number of serious challenges, such as accurate detection of the critical offset on AVO curves and computation of the corresponding critical angle at the target horizon. For models with a laterally homoge-

Seismic critical-angle reflectometry

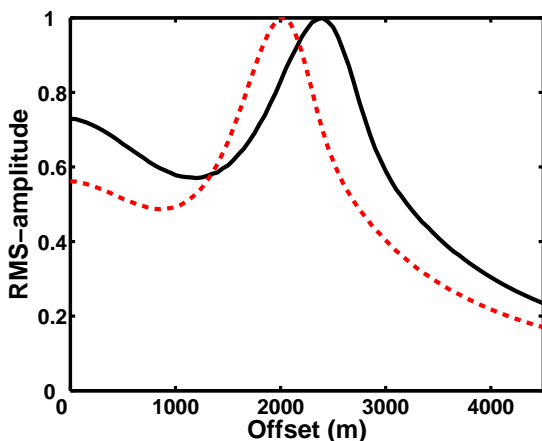


Fig. 5: Amplitude of the reflected P-wave from Figure 4 as a function of offset for the azimuths $\phi = 0^\circ$ (solid curve) and $\phi = 90^\circ$ (dashed).

neous overburden, the amplitude of the reflected wave is convenient to treat as a function of the ray parameter. At the critical offset, the ray parameter is equal to the horizontal slowness in the high-velocity layer controlled by the azimuthally varying parameter $\epsilon(\phi)$.

Conclusions

We introduced a method that can be called “seismic critical-angle reflectometry” because it is based on measuring the critical angle θ_{cr} on reflection seismic data. In contrast to AVO analysis, this method does not require accurate amplitudes for a wide offset range because the critical offset can be estimated from the point of the fastest amplitude increase.

When the medium above or below the reflector is azimuthally anisotropic, the azimuthal variation of θ_{cr} can help to constrain the symmetry-plane directions, which often coincide with the dominant fracture azimuths. Using the weak-anisotropy approximation, we obtained concise expressions for the critical angle for VTI and orthorhombic media and identified the parameter combinations that can be estimated from critical-angle reflectometry. The analytic results were verified by applying the method to the exact synthetic seismograms for the reflection from an isotropic/orthorhombic interface. The synthetic test also confirms that the extrema of the azimuthally varying function θ_{cr} do not necessarily correspond to the symmetry planes, which underscores the need for dense azimuthal coverage in critical-angle reflectometry. Currently we are analyzing the behavior of the critical angle on a field data set from the North Sea.

Acknowledgments

We are grateful to Xiaoxia Xu (CSM) for her help with the reflectivity modeling and useful suggestions. The anisotropic modeling software was developed by Dennis Corrigan (formerly of ARCO). M.L. acknowledges CSM and the Center for Wave Phenomena (CWP) for their hos-

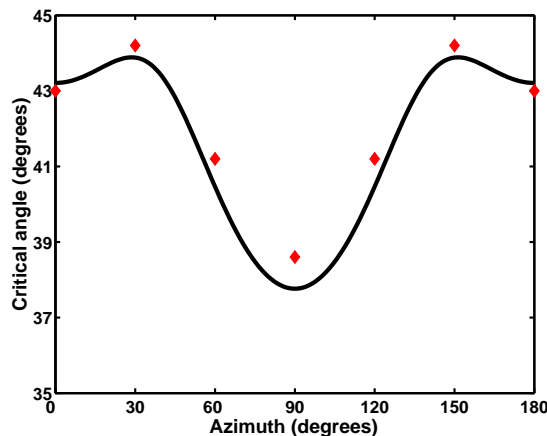


Fig. 6: Variation of the critical angle with azimuth for the model from Figure 4. The diamonds mark the critical angle estimated from the reflectivity modeling using AVO curves; the solid line is the exact critical angle.

pitality during his sabbatical visit and the Norwegian Research Council (NFR) for financial support of the ROSE (Rock Seismic) project at NTNU. This work was partially supported by the Consortium Project on Seismic Inverse Methods for Complex Structures at CWP.

References

- Antich P., and S. Mehta, 1997, Ultrasound critical-angle reflectometry (UCR): A new modality for functional elastometric imaging: *Physics in Medicine and Biology*, **42**, 1763–1777.
- Gray, F. D., G. Roberts, and K. J. Head, 2002, Recent advances in determination of fracture strike and crack density from P-wave seismic data: *The Leading Edge*, **21**, 280–285.
- Grechka, V., and I. Tsvankin, 1999, 3-D moveout inversion in azimuthally anisotropic media with lateral velocity variation: Theory and a case study: *Geophysics*, **64**, 1202–1218.
- Grechka, V., A. Pech, and I. Tsvankin, 2005, Parameter estimation in orthorhombic media using multicomponent wide-azimuth reflection data: *Geophysics*, **70**, D1–D8.
- Landrø, M., A. K. Nguyen, and H. Mehdizadeh, 2004, Time lapse refraction seismic – a tool for monitoring carbonate fields?: 74th Annual International Meeting, SEG, Expanded Abstracts, 2295–2298.
- Rüger, A., 2001, Reflection coefficients and azimuthal AVO analysis in anisotropic media: *Society of Exploration Geophysicists*.
- Tsvankin, I., 2005, *Seismic signatures and analysis of reflection data in anisotropic media*: Elsevier Science (second edition).
- Vasconcelos, I., and I. Tsvankin, 2004, Inversion of P-wave nonhyperbolic moveout in azimuthally anisotropic media: Methodology and field-data application: 74th Annual International Meeting, SEG, Expanded Abstracts, 171–174.